Additive Manufacturing 14 (2017) 31–38

Contents lists available at ScienceDirect

Additive Manufacturing

journal homepage: www.elsevier.com/locate/addma

Full length article

Closed loop control of slippage during filament transport in molten material extrusion

Gabriel Pieter Greeff*, Meinhard Schilling

Institut für Elektrische Messtechnik und Grundlagen der Elektrotechnik, Technische Universität Braunschweig, Hans-Sommer-Str. 66, D-38106 Braunschweig, Germany

ARTICLE INFO

Article history:
Received 22 September 2016
Received in revised form 27 October 2016
Accepted 25 December 2016
Available online 28 December 2016

Keywords:
Filament transport
Print quality
Feed control
Machine vision

ABSTRACT

In the quest to achieve functional 3D printed parts with open source machines and tools it is required to study all the error sources. Flow control is a major contributor to accuracy of parts manufactured additively with material extrusion and a precise filament feed rate is therefore essential. Filament slippage is measured in this work. The speed difference between filament feed gear speed and filament speed is measured with a cost effective, automated setup, using a low cost USB microscope video camera and image processing. The filament width is also measured simultaneously, allowing for real time volumetric flow rate estimation. Extrusion temperature and feed rate are found to influence the amount of slippage. Significantly, the amount of slippage varies dynamically and therefore cannot be fully corrected for statically. Proof of concept closed loop control of the extruder is also implemented and reduces the amount of slippage considerably.

1. Introduction

Functional product manufacturing with molten material extrusion (also known as FFF – Fused Filament Fabrication) especially with poly-lactic acid (PLA) is growing in popularity [1]. Such products are only feasible if the printed objects have sufficient dimensional accuracy. This accuracy requires precision of both the linear dimensions and geometry. Various static factors have been found to influence the accuracy in FFF, for example slicer settings, filament diameter, hot end nozzle diameter, geometry of the printed object and part orientation on the print bed [2].

Furthermore, the accuracy of the printed part depends on the volumetric flow rate of the extruded filament. The flow rate (extrusion rate) is determined by the pressure drop over the extruder, which depends on the liquefier geometry, filament feed rate, friction and the heat transfer dynamics. This is a function of temperature dependent material properties, such as viscosity and compressibility [3]. After extrusion, the new bead also expands (die swelling), spreads (if printed on something) and merges with previously extruded roads. Finally, the printed object can warp due to cooling effects [4].

Apart from the printing process itself, pre-process steps also affect printer accuracy. A three dimensional object is first modelled, for example by using CAD or a 3D scanner, then sliced into a command file by a slicer program and then printed. Each of these pre-process steps can introduce error, relative to the desired object. The slicer program and firmware assumes certain parameters, for example percentage over-extrusion, in order to passively correct for extrusion flow errors.

Modelling of the process helps to improve the slicer output. Closed loop control of the positioning system will further improve accuracy. For example, 75 percent trajectory error reduction was achieved by implementing closed loop control on a commercial printer [5]. Additionally, a complex three stage model for the liquefier dynamics finds a steady state volumetric flow offset and therefore recommends closed loop control of the extruder [6].

The dynamic liquefier model of [6] was verified by measuring printed tracks after extrusion was completed. In another study, the maximum sustainable extrusion speed was investigated [7]. The extruded mass was weighed and volume calculated (with the density assumed known and constant) and compared to the requested volume. The study found that the volume deviation increases with decreasing temperature. It recommends an extrusion rate limit for a 0.4 mm nozzle diameter and white PLA of around 8–10 mm^3/s. Other process monitoring techniques include acoustic emission [8], accelerometers [9] and 2D laser triangulation of the printed track [10]. A heterogeneous sensor array is implemented by [11]

* Corresponding author.
E-mail address: g.greeff@tu-bs.de (G.P. Greeff).

http://dx.doi.org/10.1016/j.addma.2016.12.005
2214-8604/

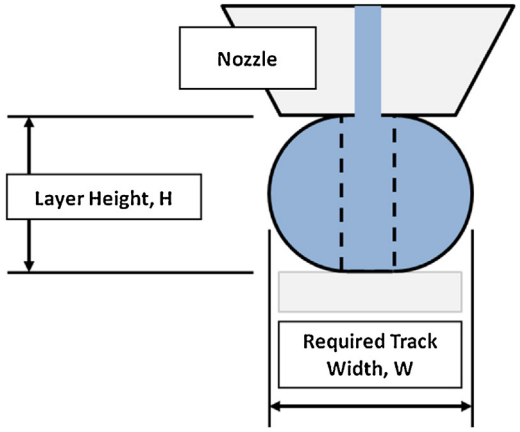

Fig. 1. Diagram of the track cross-section area approximation [17].

for online process fault detection. The sensor array includes an infrared temperature sensor for monitoring the deposited material melt pool temperature. Machine vision is used in [12] after the completion of each layer to detect extrusion errors.

The challenge is measuring actual extruder flow real time. A volumetric flow controller, patented by [13], proposes various effective filament area sensors and filament feed speed tachometers. Another control concept is presented by [14] where the motor current is used as feedback signal to detect the deposition state. Filament feed control with velocimetry is described in [15] and a liquefier with pressure sensing for feedback control is described in a patent application [16].

Eq. (1) shows that the extruded filament area A (and therefore object accuracy) depends on the track width (W) and height (H), which are determined by the volumetric flow rate (Q) divided by the feed speed (v_{feed}) [4].

$$WH = A = Q/\upsilon_{feed} \tag{1}$$

Note that the area can also be approximated with Eq. (2), by assuming that the extruded bead shape is rectangular with semi-circular edges [17], as shown in Fig. 1:

$$A = (W - H)H + \pi\left(H/2\right)^2 \tag{2}$$

The feed speed is given with Eq. (3):

$$\upsilon_{feed} = \omega_r R_r \tag{3}$$

Where R_r is the radius of the feed rollers and ω_r their angular speed. Slippage between the filament feed rollers and filament can however be induced. For example, if the force required for extruding the filament through the liquefier becomes greater than the maximum force that the feed roller can apply to the filament, then slippage can occur. Furthermore, roller roundness deviations or wear can also cause slippage. If this is not corrected for, then this slippage will lead to under-extrusion or underflow [18]. Variation in filament radius could also lead to under-extrusion [13]. Extreme filament slippage leads to filament shredding. This occurs when the filament feed rollers or extruder gear cuts into the filament, failing to push the filament into the hot end and results in complete print failure. Filament shredding also leads to flakes or shavings, which are sheared off the filament. These shavings can clog the extruder gear (increasing slippage), fall into bearings (increasing wear) or land on the print job, adversely affecting the print quality.

The design challenge with desktop printers is to improve the accuracy of the printer, without losing the cost-effective aspect of this type of printer. An advanced process model assists in this regard. If the slicer software can accurately predict the printer performance, the need for additional sensors and interfaces is reduced. A clear understanding of how the printer will react to any given G-Code command in different situations is therefore needed. Note that different printer firmware versions can interpret or execute the same command in various ways. Pressure forward compensation, for example, can be activated or a special extrusion acceleration profile implemented [19].

In this work only the extrusion command is considered. The filament slippage is investigated, defined as the filament transport speed deviation from the set point speed. Extrusion speed, filament additives (e.g. colour) and extruder temperature are investigated here to see how these variables affect filament slippage and lead to filament shredding.

2. Material and methods

A Renkforce RF1000, a desktop 3D printer, was used in this study [20]. Filament feeding can easily be visually monitored, since the filament transport mechanics is not covered in an enclosure. A USB microscope camera was mounted with 3D printed mounts and a software program developed to measure the speed of the gear and filament, as well as the filament width. Furthermore, additional software was written to control the printer, by either sending it individual G-Code commands or by starting a whole print job. This is achieved by communicating with Repetier-Server software [21] through a *Websocket* interface [22]. Automated experiments can then be performed and the results used to investigate the amount of slippage under different conditions.

The RF1000 moves the extruder in the X axis and the build table in the YZ plane. The extruder uses a metal gear mounted directly on a stepper motor; with filament clamping force provided by a spring mounted bearing (Fig. 2a and b). The extruder gear has 24 teeth and a nominal external diameter of 8 mm.

The image processing is done using the OpenCV library [23] and the Python programming language. Video frames are captured from the camera and stored. The resulting video file is then analysed. Each frame is pre-processed and certain Regions of Interest (ROIs) are then evaluated (see Fig. 2b). These ROIs are the area: (1) over the gear, (2) of filament above gear and (3) below the gear. The gear area is used to estimate the gear speed, whilst the pre-gear area is used to estimate the filament width. The filament speed is measured in the post-gear area and can also be used to analyse the pressed gear tooth profile.

2.1. Measurement uncertainty factors

A major contributor for the measurement uncertainty of the transport speed is the point displacement measurement between consecutive frames. This requires that the average time period calculated from the CPU clock is sufficiently accurate and that the actual frame rate is constant. The distance measurement depends on the camera calibration and point detection repeatability, which is also influenced by image noise. This assumes that (1) the filament is incompressible, (2) that image warping effects over small distances (6–7 pixels) are negligible, (3) that all the points tracked (on the gear and filament) are in the same plane and parallel to the camera sensor. Sub-pixel resolution however is possible with the algorithm [24]. The filament width was measured with a digital 1 μm resolution micrometer. It has a manufacturer uncertainty of ±2 μm. The magnification factor during measurements was found to be ca. 20 μm/pixel. A single micro-step, in comparison, should result in a displacement of 3.4 μm of filament. Another factor is aliasing. The time between frames was measured as (70 ± 8) ms (14.3 fps), whilst the feed rate was 280 steps/mm. It is therefore not possible to measure either a single micro-step or the micro step rate with this resolution. Fortunately, for this work, such high res-

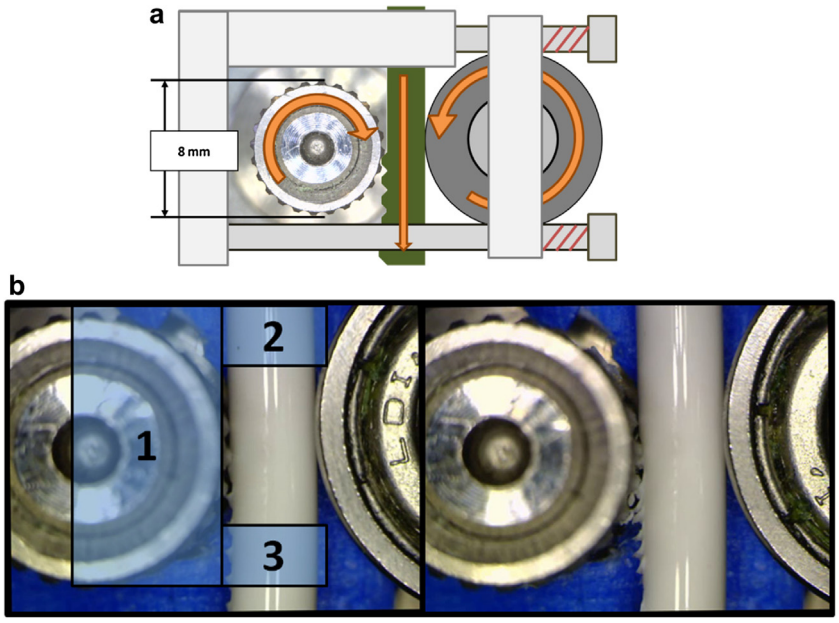

Fig. 2. a. Diagram of experimental setup with filament feed gear and spring mounted pinch bearing. b. Frames captured from microscope camera. Normal extrusion on the left with the three ROIs (Regions of Interest). Filament shredding on the right.

olution is not required and the measurement method is sufficient for the purpose of measuring filament slippage. The reason for this is the relatively longer time constant of the heat transfer dynamics in the liquefier. The relatively high frequency noise as result of resolution and aliasing can be filtered out with a low-pass filter.

The frame rate limits the maximum measurable speed to 2.5 mm/s. This not a big limitation, since this is less than the expected extrusion speeds. The current slicer settings for this printer have maximum safe print movement speed of less than 80 mm/s, which is equal to ca. 1.7 mm/s extrusion speed.

2.2. Speed estimation

The speed is estimated between consecutive frames. New, unique points to be tracked are detected at a set interval using the '*goodFeaturestoTrack*' method. These points are then used to approximate the optical flow using the Lucas-Kanade method [25]. The combination of these two methods is implemented based on an example found in standard python OpenCV distribution, which includes back calculation to select good points [24]. This process results in a series of point tracks over time per tracked point. Fig. 3 shows sequential frames after filament ROI pre-processing. The circles are an example of the positional history of the movement of a detected unique point, $P_{j,t\,x}$, during video analysis, for a track, j. The last point in the track is the newest in time.

The last two points of each track are used to determine the displacement between frames or speed in pixels per frame. These speed values are then filtered and averaged. For example, relatively large horizontal movements are removed. The speed is converted to millimetre per second by multiplying with a calibration factor and dividing with the average time step. The calibration factor (k_{cal}) is determined once for a specific setup, by measuring the width of the filament with a micrometer (w_μ) and dividing it with the width as detected by image processing ($w_{detected}$), as in Eq. (4). The detected width is determined by finding the maximum and minimum of the first derivative across the filament ROI, in the expected filament edge area. The filament width measurement is also recorded

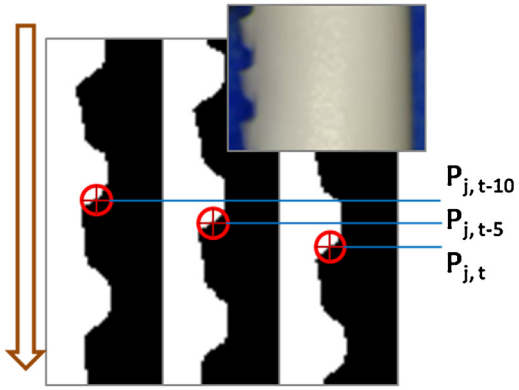

Fig. 3. Three image frames of the processed filament ROI, each 5 frames apart, with the oldest on the left and newest on the right. The circle centre indicates the movement of a unique point, P, over time for track j. The inset is the original filament ROI before processing for the first frame.

during speed measurement and can be used for volumetric flow estimation.

$$k_{cal} = w_\mu / w_{detected} \tag{4}$$

Fig. 4 shows the raw speed data as determined by the algorithm. The mean step distances of all the accepted tracked points for each frame are plotted. The gear tangential speed and the filament transport speed (v) can be calculated next with Eq. (5) with the mean step distance (S_{pxl}). The frame period is taken as the average time step between each frame ($\Delta t_{average}$) and it is measured based on the CPU clock. The speed for the time segment during gear rotation is filtered by convolving the speed with a Gaussian window (f).

$$v = f * \left(\left(k_{cal} / \Delta t_{average} \right) S_{pxl} \right) \tag{5}$$

The filtered result of the data of Fig. 4a can be seen in Fig. 4b. The red line represents the speed set point.

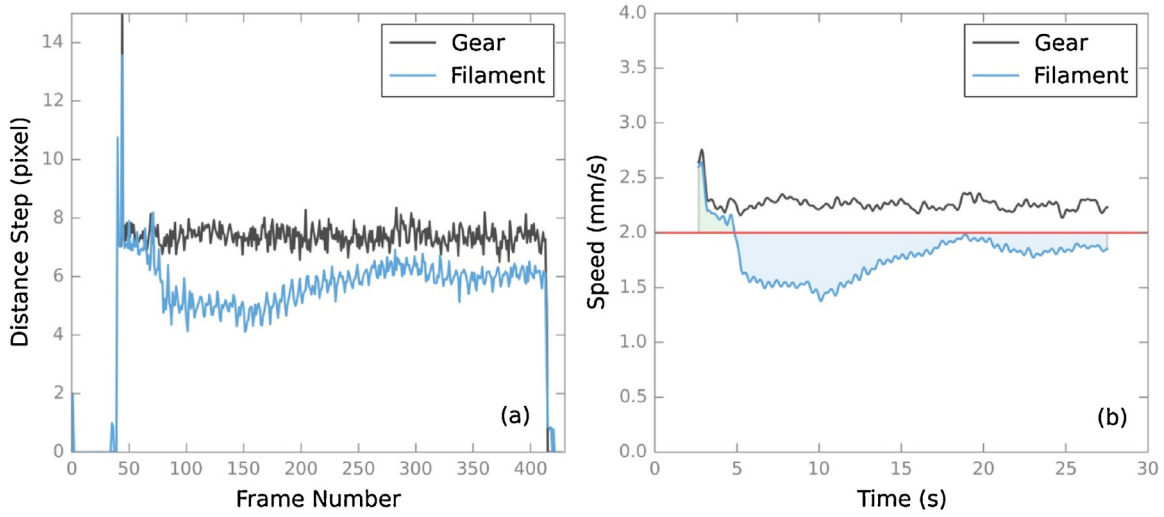

Fig. 4. (a) Example of raw speed measurement data of gear and filament speed in pixel step distance per frame number, for an extrusion of 50 mm of white PLA at 2 mm/s, at liquefier temperature of 215 °C. (b) Processing result of raw data in (a). The red line is the speed set point. (For interpretation of the references to color in this figure legend, the reader is referred to the web version of this article.)

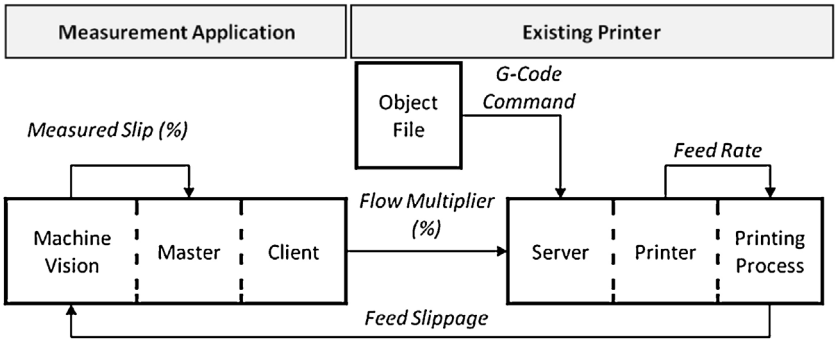

Fig. 5. Block diagram of the control process. The flow multiplier adjusts the flow and feed rate to reduce filament feed slippage.

2.3. Filament feed speed control

The server interface allows for the setting of a flow and speed rate multiplier. This is a percentage value multiplied with the G-Code command for the extruder and movement speed. Slippage, if measured real time, can therefore be used to determine a control signal, as realised with this multiply command. This method, as shown in the block diagram in Fig. 5, was used to test a proof of concept control loop for the extruder. The unmodified printer runs open loop. The server reads an object file containing the G-Codes and sends it to the printer via a communication protocol during printing. The printer interprets the G-Code command and sets the extrusion motor speed. Slippage however can now be detected by the measurement application. This program runs three threads, namely the machine vision, the master and the printer-client thread. The measured slippage in percentage, if more than a threshold, is averaged over time and used directly as the flow and feed rate multiplier. Finally, slippage is reduced by decreasing the extruder speed, after detection of filament feed slippage.

3. Results

The speed variation found in the processed speed data shown in Fig. 4b was investigated by performing three different types of experiments (1) extrusions with a specific length, temperature, material and flow rate, (2) extrusions at constant parameters, but with fixed time delays between consecutive extrusions and (3) a print job test with active control turned on or off. The hot end fan was always off during experiments and extrusion only began after the set point temperature was reached, except for the print job test. All extrusions were made with a 0.5 mm nozzle and the filament was fed from the filament roller supplied by the manufacturer.

3.1. Influence of filament material additives (Colour), diameter, temperature and speed

The multiple test extrusions, performed with three different material additives (filament colours) at three extrusion speeds over a temperature range, are used to investigate the influence of these parameters on filament transport slippage.

Green coloured PLA filament (procured from *Conrad Electronic* [20]), with a nominal diameter of 3 mm, white coloured 2.85 mm PLA filament and a clear or natural 2.85 mm PLA were used. The 2.85 mm filaments were procured from *Das Filament* [26]. The manufacturers recommend an extrusion temperature of 215 °C. A temperature range of 185 °C to 230 °C with 5° C steps was therefore selected. A length of 50 mm was extruded each time.

The speed deviation from the set point as requested by the G-Code command for the three different material colours (also at three different speeds) were measured and are shown in Fig. 6. Here slippage increases with decreasing temperature and with increasing speed. The larger diameter green filament achieved the lowest sustainable extrusion temperature at 185 °C with less than 20% slippage at 1.5 mm/s. The smaller diameter (clear and white coloured)

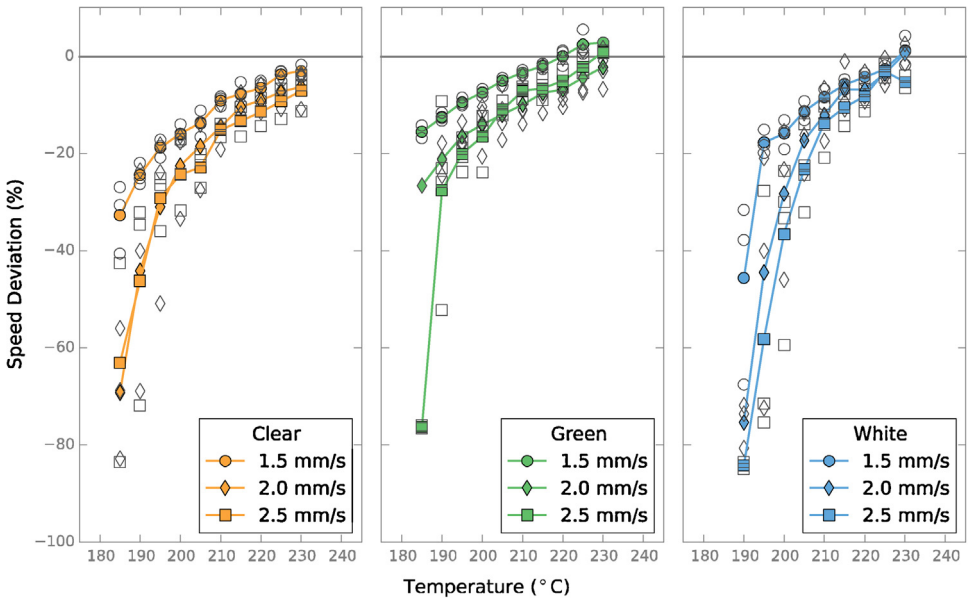

Fig. 6. Speed deviation percentage for each of the three tested filaments at three different speeds. Solid lines and filled markers indicate average speed deviation (at every temperature point, for each speed) and open symbols the individual extrusions.

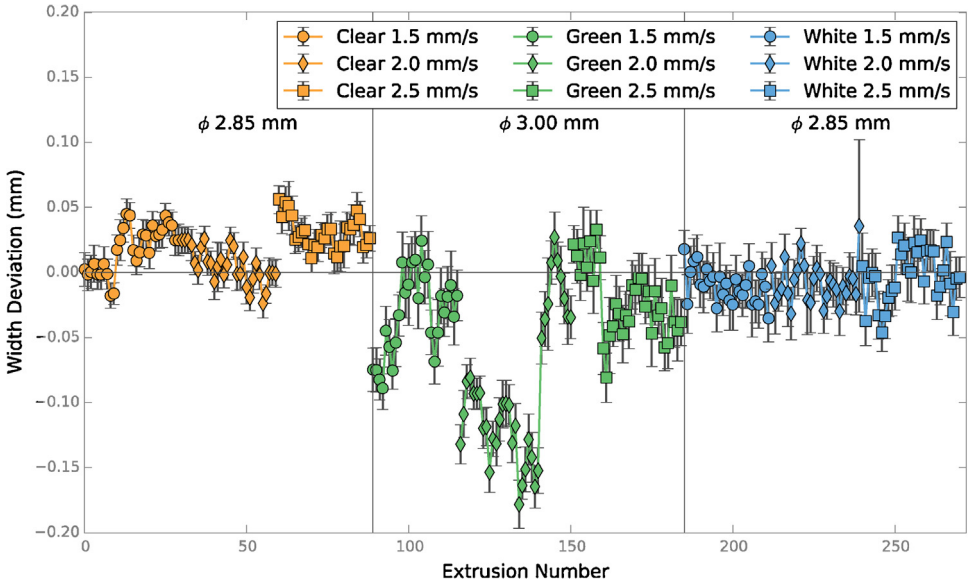

Fig. 7. Chronologically sorted (per material) filament width deviation for each extrusion (for each of the three tested filaments at three different speeds); the error bars indicate the standard deviation during the extrusion.

filament extrusion however could only go down to 195 °C, before starting to fail. Here extrusion failure, i.e. cutting into filament, is more likely to occur at temperatures below 200 °C. The 215 °C recommended temperature resulted in under-extrusion of around 10% for all three filaments. This agrees with findings of [6,7] where under-extrusion was also measured.

These results confirm that slippage is dependent on temperature and extrusion speed. Note however that the larger filament (3 mm diameter) will have a larger surface area and smaller air gap between the filament and liquefier. This should reduce the thermal resistance as postulated in [3] and therefore reduce the pressure drop in the first liquefier zone. Filament material also has a smaller effect, which is seen by comparing the clear filament and the white filament results.

The length of filament fed into the extruder is calculated next by integrating the speed measured for each extrusion. The volume of material fed into the liquefier is determined subsequently, using the measured filament width. The average measured width deviation from the manufacturer supplied diameter per extrusion is plotted in Fig. 7. The width value is used as an approximation for the filament diameter, assuming perfect roundness. The standard deviation per extrusion is in the range of the camera resolution (around 20 μm). Nevertheless, the green filament exhibited a larger variation than the clear and white coloured filament.

Fig. 8 combines the length and diameter information, to determine the volume deviation percentage for the three filaments. Under-extrusion is always present at temperatures less than 230 °C and at extrusion speeds faster than 1.5 mm/s. It is also clear that temperature and speed variation can influence the extruded volume. The amount of under-extrusion is also not constant.

Slicer software allows users to correct under-extrusion with a set amount of over-extrusion (a percentage value for example). This

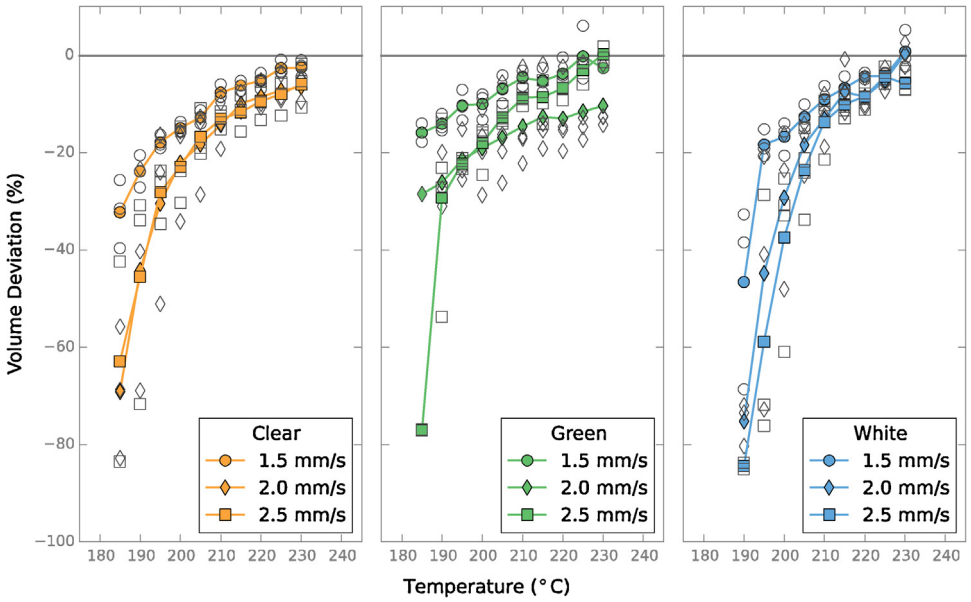

Fig. 8. Volume deviation percentage for each of the three tested filaments at three different speeds. Solid lines and filled markers indicate average volume deviation (at every temperature point, for each speed) and open symbols the individual extrusions.

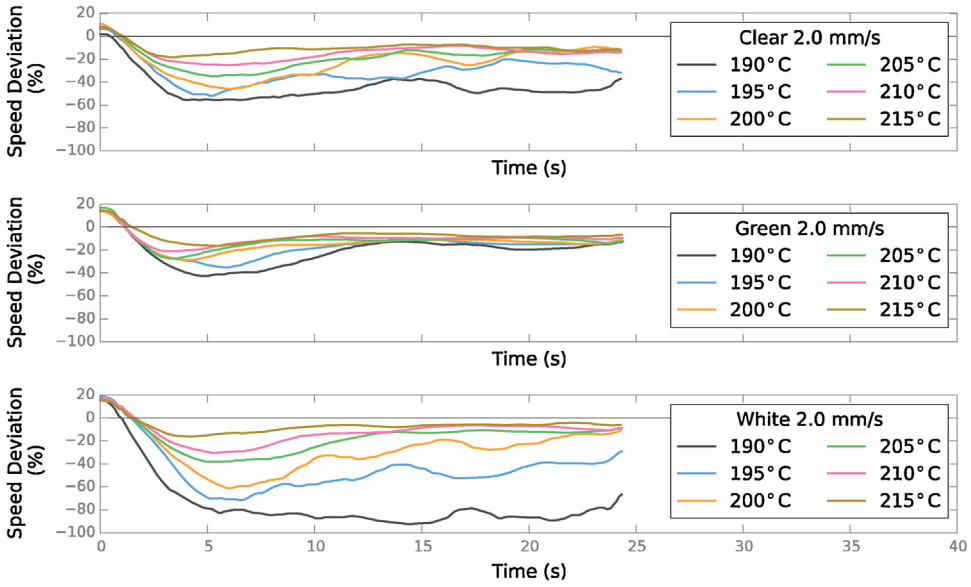

Fig. 9. Average speed deviation profile at a specific temperature, for an extrusion speed of 2 mm/s, with three different materials.

however will not compensate for dynamic effects. Fig. 9 plots the speed profile average per temperature set point, for the 2 mm/s speed. The slippage development over time depends on both extrusion speed and temperature. Extrusion failure is found at 190 °C for the white filament. A maximum point at around 5 s and a semi-steady state after 15 s can also be distinguished. The time dependence of the slippage shows non-constant filament transport speed, which can lead to variation in extrusion width, which in turn is not corrected with static slicer settings.

3.2. Influence of time delay and retraction

The average slippage percentage over time for the time gap test is shown in Fig. 10. During these experiments a sequence of extrusions was made, after heating the extruder to 200 °C from below the glass transition temperature T_g (55 °C). Two sets of six measurements were taken. One set without retraction and the other with retraction. Interestingly, heating from below T_g influences the slippage, in that it is different from the subsequent, time delayed, extrusions. Retraction is also seen to slightly increase the amount of slippage and the variation.

3.3. Print job test

The final result is the print job test. Here a single track width polygon is printed. The polygon has 40 sides and each side is about 5.3 mm long. The hollow object is 10 mm tall and requires 33 layers with a layer thickness of 0.3 mm. The first 11 layers were printed at 230 °C, the next 11 at 190 °C and the last layers again at 230 °C to demonstrate the influence of slippage during the printing process.

Fig. 11 compares the percentage slip, relative to gear speed, during the print job test. The amount of slip is only shown for periods of gear movement and filtered to increase readability. The extruder temperature is also plotted. The printer first waited for the extruder

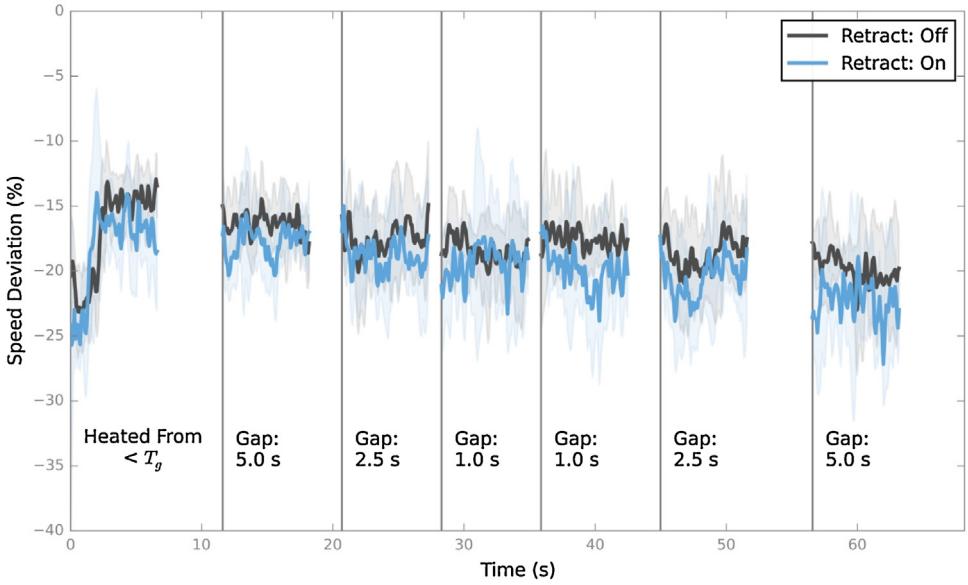

Fig. 10. Result of the extrusion gap test with white filament. Waiting periods are not shown and text annotation indicate time before extrusion began. Extrusion temperature is 200 °C, length 15 mm, speed 2 mm/s. Retraction: speed 16 mm/s and 1 mm length. Shaded areas show the standard deviation per set.

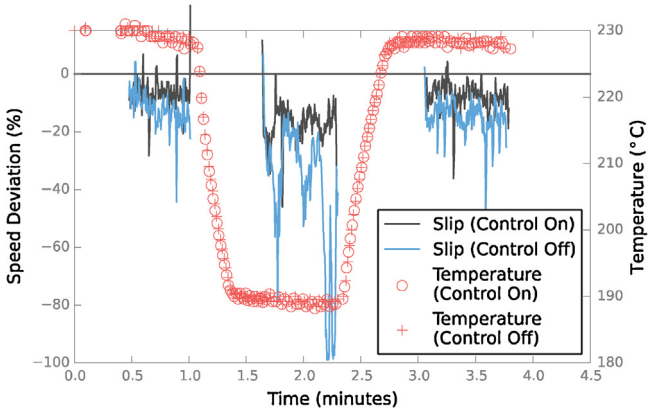

Fig. 11. Speed deviation percentage for the job print test, with control on and off. The temperature for each print is plotted on the secondary axes. The test with the control turned off is failing to extrude, after about 2 minutes of printing.

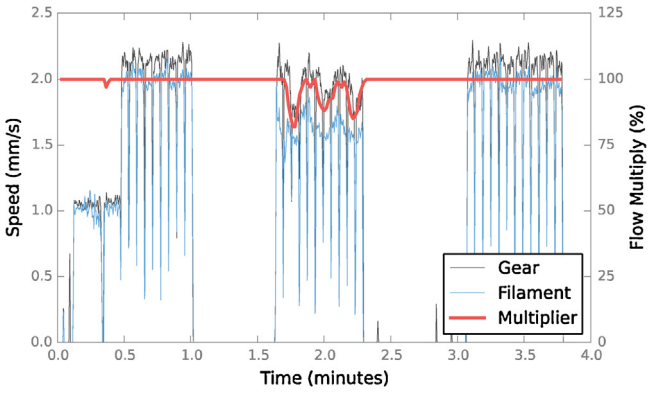

Fig. 12. Gear and filament speed with control activated. The multiplier percentage is plotted on the secondary axis. The gear speed adapts to reduce filament slippage.

to reach the set point temperature, before continuing the print. Slippage increases as expected in the middle segment of the three layer sets. The control loop based on the optically measured speed reduces gear speed in order to reduce slip, also works as desired by significantly improving the print.

The flow and speed multiplier slows the printer down or speeds it up. The multiplier value, as sent to the printer during the active control print test, is shown in Fig. 12. The gear speed and filament speed are depicted as well. The sharp vertical spikes are filament retractions between layers. The printer first prints an extruder test line and then the first layer at a slower speed of 1 mm/s. The remainder is printed at a set point speed of 2 mm/s. The gear speed is seen to follow the multiplier value, specifically in the middle section at the lower extrusion temperature.

Fig. 13 is a photo of the two printed polygons. The left object was printed with control turned off and the resulting under-extrusion is self-evident. This test was repeated twice and the four objects were weighed. The repeatability of the test was gauged by comparing the mass of the objects. The difference was (0.030 ± 0.001) g with control-on and (0.021 ± 0.001) g for the objects with the control turned off. The average difference in mass, between the control-off and control-on test objects, was found to be (0.198 ± 0.001) g. This is equal to a 14% mass increase by turning the control on. The job print test with active extruder flow rate control confirms, for the speed range and materials used, that (1) implementing closed loop control reduces slippage, (2) slippage is less at lower speeds, (3) slippage is also lower at higher temperatures and (4) that there is slippage variation during printing.

4. Discussion and conclusion

Slippage, the difference between filament transport speed and set point feed speed, is measured with a cost effective, open source solution. Filament feed slippage is the result of insufficient grip of extruder feed gear on the filament. The amount of grip required depends on the pressure drop over the liquefier. The pressure drop dynamics is also complicated by temperature dependent material properties and filament feed speed variation.

Slippage increases with decreasing temperature and with increasing speed. This can lead to extruded track width variation, which in turn causes functional and dimensional errors. The actual extruder pressure should be considered however, before a final conclusion regarding actual extruded volumetric flow rate can be made. Nevertheless, it is expected that filament transport speed in steady state will directly set extrusion flow rate.

Fig. 13. Photo of the two print job tests. Each object is a 40 sided polygon with a diameter of 68 mm. The left object was printed with control turned off and the right with control turned on. Large blobs on the wall are the positions where the extruder waited until the temperature reached a new set point.

Tests during printing of an object, as well as tests investigating the effect of retraction were performed and found that the slippage effect occurs during normal printing. Slicer software does allow a user to statically correct under-extrusion with a set amount of over-extrusion (a percentage value for example). Users should however note that the results of this study show the amount of slippage varies with speed and temperature. Furthermore, it was found that slippage depends on extrusion history.

Filament shredding can occur if the force required becomes too high, leading to print failure. This shredding can be reduced by increasing filament diameter, increasing temperature and decreasing speed. Increasing temperature can however lead to other printing related problems, such as stringing or extruder oozing. Alternatively, decreasing the speed will increase printing time. Self optimisation or calibration is therefore required to determine the optimum parameters for each print job and filament combination. The sustainable maximum speed (to decrease printing time) and optimal temperature for each filament can be determined. It remains to be answered what the relative contribution of filament material and extruder design on filament transport slippage is. Additionally, standardised quality tests and parameters for filaments will also be valuable.

It is therefore feasible that slicer models can be fine tuned, by setting the over-extrusion parameters and so forth, but a closed loop control system is ultimately required for higher accuracy. In order to achieve such a control system detailed knowledge of the transfer function is essential. A proof of concept control system is however implemented and tested here and shown to significantly improve the printed objects.

Acknowledgements

We gratefully acknowledge support by the Braunschweig International Graduate School of Metrology (B-IGSM) and the National Metrology Institute of South Africa (NMISA).

References

[1] B. Wittbrodt, J.M. Pearce, The effects of PLA color on material properties of 3-D printed components, Addit. Manuf. 8 (2015) 110–116, http://dx.doi.org/10.1016/j.addma.2015.09.006.
[2] P. Lee, H. Chung, S.W. Lee, J. Yoo, J. Ko, Review: dimensional accuracy in additive manufacturing processes, Mater. Micro Nano Technol. Prop. Appl. Syst. Sustain. Manuf. 1 (2014), http://dx.doi.org/10.1115/msec2014-4037, pp. V001T04A045.
[3] B.N. Turner, R. Strong, S.A. Gold, A review of melt extrusion additive manufacturing processes: I. Process design and modeling, Rapid Prototyping J. 20 (2014) 192–204, http://dx.doi.org/10.1108/RPJ-01-2013-0012.
[4] B.N. Turner, S.A. Gold, A review of melt extrusion additive manufacturing processes: II. Materials, dimensional accuracy, and surface roughness, Rapid Prototyping J. 21 (2015) 250–261, http://dx.doi.org/10.1108/RPJ-02-2013-0017.
[5] B. Weiss, D.W. Storti, M.A. Ganter, Low-cost closed-loop control of a 3D printer gantry, Rapid Prototyping J. 21 (2015) 482–490, http://dx.doi.org/10.1108/RPJ-09-2014-0108.
[6] A. Bellini, S. Güçeri, M. Bertoldi, Liquefier dynamics in fused deposition, J. Manuf. Sci. Eng. 126 (2004) 237, http://dx.doi.org/10.1115/1.1688377.
[7] S.J. Oliver, Extrudable Me! Exploring Extrusion Variability and Limits, (2013). http://www.extrudable.me/2013/04/18/exploring-extrusion-variability-and-limits/ (Accessed 21 June 2016).
[8] H. Wu, Y. Wang, Z. Yu, In situ monitoring of FDM machine condition via acoustic emission, Int. J. Adv. Manuf. Technol. (2015), http://dx.doi.org/10.1007/s00170-015-7809-4.
[9] S. Bukkapatnam, B. Clark, Dynamic modeling and monitoring of contour crafting—an extrusion-based layered manufacturing process, J. Manuf. Sci. Eng. 129 (2007) 135, http://dx.doi.org/10.1115/1.2375137.
[10] M. Faes, W. Abbeloos, F. Vogeler, C.K.H. Valkenaers, T. Goedeme, E. Ferraris, Process monitoring of extrusion based 3D printing via laser scanning, Int. Conf. Polym. Mould. Innov. (2014) PMI2014, http://dx.doi.org/10.13140/2.1.5175.0081.
[11] P.K. Rao, J. (Peter) Liu, D. Roberson, Z. (James) Kong, C. Williams, Online real-time quality monitoring in additive manufacturing processes using heterogeneous sensors, J. Manuf. Sci. Eng. 137 (2015) 61007, http://dx.doi.org/10.1115/1.4029823.
[12] T. Fang, M.A. Jafari, S.C. Danforth, A. Safari, Signature analysis and defect detection in layered manufacturing of ceramic sensors and actuators, Mach. Vis. Appl. 15 (2003) 63–75, http://dx.doi.org/10.1007/s00138-002-0074-1.
[13] R.L. Zinniel, J.S. Batchelder, Volumetric Feed Control for Flexible Filament, US 6085957, 2000.
[14] C. Kim, D. Espalin, A. Cuaron, M.A. Perez, E. MacDonald, R.B. Wicker, A study to detect a material deposition status in fused deposition modeling technology, IEEE Int. Conf. Adv. Intell. Mechatronics, IEEE, 2015 (2015) 779–783, http://dx.doi.org/10.1109/AIM.2015.7222632.
[15] J.S. Batchelder, Additive Manufacturing System and Method for Printing Three-Dimensional Parts Using Velocimetry, US 2014/0044692 A1, 2014.
[16] J.S. Batchelder, W.J., Swanson, K.C. Johnson, Additive Manufacturing System and Process with Material Flow Feedback Control, US 2015/0097308A1, 2013.
[17] G. Hodgson, A. Ranellucci, J. Moe, Slic3r Manual – Flow Math, 2016 (Accessed 21 June 2016) http://manual.slic3r.org/advanced/flow-math.
[18] M.K. Agarwala, V.R. Jamalabad, N. a. Langrana, A. Safari, P.J. Whalen, S.C. Danforth, Structural quality of parts processed by fused deposition, Rapid Prototyping J. 2 (1996) 4–19, http://dx.doi.org/10.1108/13552549610732034.
[19] Repetier, Hardware settings and print quality, (2011). https://github.com/repetier/Repetier-Firmware/wiki/Hardware-settings-and-print-quality (Accessed 19 September 2016).
[20] Renkforce RF1000 3D Drucker, Conrad Electronic, (2016). https://www.conrad.de/de/renkforce-rf1000-3d-drucker-single-extruder-inkl-software-franzis-designcad-v24-3d-print-renkforce-edition-1007508.html (Accessed 20 September 2016).
[21] Repetier, Repetier-Server API description, (2016). https://www.repetier-server.com/manuals/programming/API/index.html (Accessed 20 September 2016).
[22] Open-source real-time framework for Web, Mobile & Internet of Things, (2016). http://autobahn.ws/ (Accessed 20 September 2016).
[23] Itseez, Open Source Computer Vision Library, (2015).
[24] A. Mordvintsev, K. Abid, Optical Flow Tutorial, 2013 (Accessed 26 October 2016) http://opencv-python-tutroals.readthedocs.io/en/latest/py_tutorials/py_video/py_lucas_kanade/py_lucas_kanade.html.
[25] J.-Y. Bouguet, Pyramidal implementation of the affine Lucas Kanade feature tracker description of the algorithm, Intel Corp. 5 (2001) 4.
[26] Das Filament (2016). https://www.dasfilament.de/ (Accessed 20 September 2016).